Tunneling of a diatomic molecule with unbound states in one dimension

Mark R. A. Shegelski, Jeff Hnybida, Hal Friesen, Crystal Lind, and Jeremy Kavka
Department of Physics, University of Northern British Columbia, Prince George, British Columbia, Canada V2N 4Z9
(Received 17 December 2007; published 5 March 2008)

We study the reflection and transmission of a homonuclear diatomic molecule incident upon a potential barrier in one dimension. The effect of discrete and continuous unbound molecular states is investigated. We use the method of variable reflection and transmission amplitudes for discrete unbound states and we extend the method to include continuous unbound states. We take into account transitions between the bound and unbound states in the process of tunneling. For the molecule incident in a bound state, we calculate the probabilities of reflection and transmission in bound states as well as in unbound states. We focus on the molecule incident upon a δ barrier but we also investigate rectangular and Gaussian barriers. We show that transmission resonances are appreciably reduced by the inclusion of unbound states due to the lack of resonant structure in the probabilities of reflection and transmission in unbound states. We also find that much of the behavior of the molecule in the process of tunneling is primarily due to the bound states.

DOI: 10.1103/PhysRevA.77.032702 PACS number(s): 34.20.Cf, 03.65.Xp, 34.20.Gj, 34.50.Bw

I. INTRODUCTION

Technological advancements have expanded the study of tunneling phenomena in quantum mechanics and have generated a number of experimental applications, including, for example, the tunneling of a single hydrogen atom on a metal surface, which was observed directly by Lauhon and Ho using a scanning tunneling microscope [1]. More exotic examples include the resonant tunneling of Cooper pairs [2] and the direct observation of tunneling in a single bosonic Josephson junction [3]. The tunneling of molecules and other composite particles is a fairly new area of research. The resonant tunneling of a pair of bound particles incident upon a single barrier was studied by Saito and Kayanuma [4]. Pen'kov continued this work by studying more general barriers and by providing a mechanism for the appearance of resonances [5,6]. Anomalously high resonant tunneling of a pair of bound particles in a one-dimensional lattice was studied by Bulatov and Kornilovitch [7]. Further, Bertulani, Flambaum, and Zelevinsky showed that the probability of tunneling of a pair of bound particles is greatly affected by the intrinsic structure (e.g., spin) of the pair [8]. More relevant to this article, Bacca and Feldmeier [9] as well as Lee [10] have also studied the resonant tunneling of a pair of bound particles. However, the binding potential used in these two studies is more applicable to nuclear physics. What has not been investigated in previous studies, but is reported here, are the implications of molecular break-up for the tunneling or reflection of a molecule incident upon a potential barrier.

Tunneling of a diatomic molecule incident upon a potential barrier in one and three dimensions was reported in Refs. [11] and [12], respectively. The work in one dimension used a binding potential which allowed for transitions between the bound states during the process of tunneling. We expand on this work by including unbound states for the same binding potential as in Ref. [11] and allowing for transitions between any of the bound and unbound states. Using an elegant method developed by Razavy [13], we investigate the tunneling of a molecule having discrete unbound states. We then extend the method to the case of continuous unbound states. For a molecule incident in a bound state, we calculate the probabilities of reflection and transmission in bound states as well as in unbound states.

We find that the transmission resonances are appreciably reduced by the inclusion of unbound states and that the behavior of the molecule in the process of tunneling is mainly due to the bound states. We also show that use of a large number of discrete unbound states does not provide adequate information to deduce the behavior of a molecule with a continuum of unbound states. We focus on the probabilities of tunneling through a δ barrier, but we also investigate rectangular and Gaussian barriers. We provide physical explanations for our results and discuss extensions to more realistic systems and experimental studies in molecular physics.

II. FORMULATION OF THE PROBLEM

We study the transmission and reflection of a homonuclear diatomic molecule of mass $2m$ incident upon a potential barrier in one dimension. Choosing x_1 and x_2 to be the spatial coordinates of the two atoms, the Hamiltonian is given by

$$H = -\frac{\hbar^2}{2m}\left(\frac{\partial^2}{\partial x_1^2} + \frac{\partial^2}{\partial x_2^2}\right) + V(x_1) + V(x_2) + V_0(x_1 - x_2), \quad (1)$$

where $V(x_j)$ (for $j=1,2$) is the potential barrier and $V_0(x_1 - x_2)$ is the binding potential. By defining $\xi \equiv x_1 - x_2$ and $x \equiv \frac{1}{2}(x_1 + x_2)$ we replace the two-particle coordinates x_1 and x_2 by relative and center-of-mass coordinates ξ and x. With this transformation the Hamiltonian becomes

$$H = -\frac{\hbar^2}{2m}\left(\frac{1}{2}\frac{\partial^2}{\partial x^2} + 2\frac{\partial^2}{\partial \xi^2}\right) + V\left(x + \frac{1}{2}\xi\right) + V\left(x - \frac{1}{2}\xi\right) + V_0(\xi). \quad (2)$$

The amount of numerical work required to calculate the probabilities of reflection and transmission of the molecule can be considerably reduced by employing the method of

variable reflection and transmission amplitudes developed by Razavy [13]. This method allows us to calculate the coefficients of reflection and transmission without having to calculate the actual wave function of the molecule. In using this method, the total wave function of the molecule is expanded in terms of the relative motion eigenfunctions. For a molecule with bound and unbound states, the molecule's wave function $\Psi(x,\xi)$ has the form

$$\Psi(x,\xi) = \sum_n \psi_n(x)\chi_n(\xi) + \int dq \psi_q(x)\chi_q(\xi), \tag{3}$$

where $\chi_n(\xi)$ and $\chi_q(\xi)$ are the bound and unbound relative motion eigenfunctions of the molecule, respectively.

We choose $\chi_n(\xi)$ and $\chi_q(\xi)$ to satisfy the relative motion Schrödinger equation with binding Hamiltonian H_b:

$$H_b\chi_n(\xi) = \left(-\frac{\hbar^2}{m}\frac{d^2}{d\xi^2} + V_0(\xi)\right)\chi_n(\xi) = e_n\chi_n(\xi), \tag{4}$$

$$H_b\chi_q(\xi) = \left(-\frac{\hbar^2}{m}\frac{d^2}{d\xi^2} + V_0(\xi)\right)\chi_q(\xi) = e_q\chi_q(\xi), \tag{5}$$

where $e_n<0$ and $e_q>0$ are the energies of the bound and unbound states. In these expressions, "n" labels bound states and "q" labels unbound states.

Razavy's method applies to a set of discrete states, whereas the wave function given in Eq. (3) contains a continuum of unbound states. We extend Razavy's method to a continuum of states in two steps. First, we take the binding potential to confine the atoms to a finite range of length $2L$, which gives a discrete set of unbound states. Then we take $L\to\infty$ to obtain a continuum of unbound states. This turns out to be much easier than attempting to extend Razavy's method to the continuum of unbound states in a single step.

An alternative approach would be to use the time-dependent Schrödinger or Lippmann-Schwinger equation and represent the molecule by a wave packet. One could then calculate the time evolution of the wave packet and obtain the probabilities of transmission and reflection. Jackson presented a review [14] explaining such an approach, using a Fourier grid for the packet to study chemical reaction dynamics, and noted that a physical and intuitive picture can be obtained using time-dependent methods. Use of wave packets and a treatment along these lines could apply to the problem studied here; it would be straightforward to extend this to three dimensions.

A. Discrete unbound states

If we restrict the range of the binding potential to a finite length L, the unbound states become discrete, i.e., the energies e_q are discrete. The binding potential has the general form

$$V_0(\xi) = \begin{cases} V_0'(\xi), & |\xi| < L, \\ \infty, & |\xi| > L, \end{cases} \tag{6}$$

where $V_0'(\xi)$ is a suitable choice for a molecular potential.

For discrete unbound states, the integral in Eq. (3) is replaced by a sum. For brevity we will express the sum over bound states and the sum over unbound states, in the wave function of the molecule, by a single sum over all bound and unbound states

$$\Psi(x,\xi) = \sum_\phi \psi_\phi(x)\chi_\phi(\xi). \tag{7}$$

Henceforth, Greek letter indices will be used to index both bound and unbound states. Substituting Eq. (7) into Schrödinger's equation $H\Psi(x,\xi)=E\Psi(x,\xi)$, multiplying on the left by $\chi_\mu^*(\xi)$, and integrating over ξ, we obtain

$$\left(\frac{d^2}{dx^2} + k_\mu^2\right)\psi_\mu(x) - \sum_\phi z_{\mu\phi}(x)\psi_\phi(x) = 0, \tag{8}$$

where $z_{\mu\nu}(x)$ is defined by

$$z_{\mu\nu}(x) \equiv \frac{4m}{\hbar^2}\int_{-\infty}^{\infty}\left[V\left(x+\frac{1}{2}\xi\right) + V\left(x-\frac{1}{2}\xi\right)\right]\chi_\mu^*(\xi)\chi_\nu(\xi)d\xi, \tag{9}$$

and the center-of-mass wave numbers are defined by

$$k_\mu^2 = \frac{4m}{\hbar^2}(E - e_\mu). \tag{10}$$

The problem has been reduced to a set of differential equations in a form known as the "multichannel" Schrödinger equation.[1] In this form, the center-of-mass motion can be studied while the effect of the relative motion is entirely contained in the "effective" potentials $z_{\mu\nu}(x)$. Moreover, each effective potential $z_{\mu\nu}(x)$ can be thought of as the potential barrier that the center-of-mass encounters while incident in state μ and reflected or transmitted in state ν.

The form of Eq. (8) with bound and discrete unbound states (Greek indices) is identical to Eq. (7) of Ref. [11], in which only bound states were considered. Therefore the transformation of Eq. (8), via the method of variable reflection and transmission amplitudes, will have the same form as Eq. (7) in Ref. [11], except with Greek indices. Note that this method involves writing the coefficients $R_{\mu\nu}$ and $T_{\mu\nu}$ in terms of a variable y in which the limit $y\to-\infty$ yields the true coefficients of reflection and transmission. The sets of coupled differential equations produced using the method are as follows:[2]

$$\frac{d}{dy}R_{\mu\nu}(y) = -\sum_\phi \frac{1}{2ik_\phi}[e^{ik_\phi y}\delta_{\mu\phi} + e^{-ik_\phi y}R_{\mu\phi}(y)] \times \sum_\gamma z_{\phi\gamma}(y)[e^{ik_\gamma y}\delta_{\gamma\nu} + e^{-ik_\gamma y}R_{\gamma\nu}(y)], \tag{11}$$

[1] See Ref. [13], Chap. 11, pp. 205–215.

[2] There is a typographical error in Eq. (17) for $T_{\mu\nu}$ in Ref. [11]. The correct equation is given in this article as Eq. (12).

$$\frac{d}{dy}T_{\mu\nu}(y) = -\sum_{\phi}\frac{1}{2ik_{\phi}}e^{-ik_{\phi}y}T_{\mu\phi}(y) \times\sum_{\gamma} z_{\phi\gamma}(y)[e^{ik_{\gamma}y}\delta_{\gamma\nu} + e^{-ik_{\gamma}y}R_{\gamma\nu}(y)], \quad (12)$$

subject to the boundary conditions

$$R_{\mu\nu}(y\to\infty) = 0, \quad R_{\mu\nu}(y\to-\infty) = R_{\mu\nu}, \quad (13)$$

$$T_{\mu\nu}(y\to\infty) = \delta_{\mu\nu}, \quad T_{\mu\nu}(y\to-\infty) = T_{\mu\nu}, \quad (14)$$

where $R_{\mu\nu}$ and $T_{\mu\nu}$ are the true coefficients of reflection and transmission. Due to the complexity of the effective potentials we will use a Runge-Kutta method [15] to solve these sets of coupled differential equations numerically.

The total probabilities of reflection and transmission in a bound state for a molecule incident in the state ν are readily shown to be

$$p_{\mathrm{RB}}^{(\nu)} = \sum_{n}\frac{k_n}{k_\nu}|R_{n\nu}|^2, \quad (15)$$

$$p_{\mathrm{TB}}^{(\nu)} = \sum_{n}\frac{k_n}{k_\nu}|T_{n\nu}|^2, \quad (16)$$

where n indexes all bound states. Similarly, the total probabilities of reflection and transmission in an unbound state for a molecule incident in the state ν are

$$p_{\mathrm{RU}}^{(\nu)} = \sum_{q}\frac{k_q}{k_\nu}|R_{q\nu}|^2, \quad (17)$$

$$p_{\mathrm{TU}}^{(\nu)} = \sum_{q}\frac{k_q}{k_\nu}|T_{q\nu}|^2, \quad (18)$$

where q indexes all unbound states. The total probabilities of reflection and transmission are

$$p_R^{(\nu)} = p_{\mathrm{RB}}^{(\nu)} + p_{\mathrm{RU}}^{(\nu)}, \quad (19)$$

$$p_T^{(\nu)} = p_{\mathrm{TB}}^{(\nu)} + p_{\mathrm{TU}}^{(\nu)}. \quad (20)$$

We also have

$$p_{\mathrm{RB}}^{(\nu)} + p_{\mathrm{TB}}^{(\nu)} + p_{\mathrm{RU}}^{(\nu)} + p_{\mathrm{TU}}^{(\nu)} = 1. \quad (21)$$

B. Continuous unbound states

Taking the $L\to\infty$ limit in Eq. (6) results in a continuum of unbound state energies $e_q = \hbar^2q^2/m$. Consequently, each sum over a set of unbound states must be converted to an integral. The separation between successive unbound state wave numbers, over which the integrations are performed, approaches π/L.

Dirac δ terms arising from the Kronecker δ terms in the differential equations for $R_{\mu\nu}$ and $T_{\mu\nu}$, as well as in the boundary conditions, pose a significant problem when solving the equations numerically. This problem can be avoided by defining the intermediary quantities $U_{\mu\nu}(y)$ and $Q_{\mu\nu}(y)$ before taking the $L\to\infty$ limit. $U_{\mu\nu}(y)$ and $Q_{\mu\nu}(y)$ are defined as follows:

$$R_{\mu\nu}(y) \equiv 2ik_\nu U_{\mu\nu}(y)e^{i(k_\mu+k_\nu)y}, \quad (22)$$

$$T_{\mu\nu}(y) \equiv 2ik_\nu Q_{\mu\nu}(y)e^{i(k_\mu+k_\nu)y} + \delta_{\mu\nu}. \quad (23)$$

The resulting sets of differential equations are

$$\begin{aligned}\frac{d}{dy}U_{\mu\nu}(y) = &-i(k_\mu+k_\nu)U_{\mu\nu}(y) - \sum_j\sum_m U_{\mu j}(y)z_{jm}(y)U_{m\nu}(y)\\ &-\frac{1}{\pi}\sum_j\int dpU_{\mu j}(y)z_{jp}(y)U_{p\nu}(y)\\ &-\frac{1}{\pi}\int ds\sum_m U_{\mu s}(y)z_{sm}(y)U_{m\nu}(y)\\ &-\frac{1}{\pi^2}\int ds\int dpU_{\mu s}(y)z_{sp}(y)U_{p\nu}(y)\\ &-\frac{1}{2ik_\nu}\sum_j U_{\mu j}(y)z_{j\nu}(y) - \frac{1}{2\pi ik_\nu}\int dsU_{\mu s}(y)z_{s\nu}(y)\\ &-\frac{1}{2ik_\mu}\sum_m z_{\mu m}(y)U_{m\nu}(y)\\ &-\frac{1}{2\pi ik_\mu}\int dpz_{\mu p}(y)U_{p\nu}(y) - \frac{1}{2ik_\mu}\frac{1}{2ik_\nu}z_{\mu\nu}(y),\end{aligned} \quad (24)$$

$$\begin{aligned}\frac{d}{dy}Q_{\mu\nu}(y) = &-i(k_\mu+k_\nu)Q_{\mu\nu}(y) - \sum_j\sum_m Q_{\mu j}(y)z_{jm}(y)U_{m\nu}(y)\\ &-\frac{1}{\pi}\sum_j\int dpQ_{\mu j}(y)z_{jp}(y)U_{p\nu}(y)\\ &-\frac{1}{\pi}\int ds\sum_m Q_{\mu s}(y)z_{sm}(y)U_{m\nu}(y)\\ &-\frac{1}{\pi^2}\int ds\int dpQ_{\mu s}(y)z_{sp}(y)U_{p\nu}(y)\\ &-\frac{1}{2ik_\nu}\sum_j Q_{\mu j}(y)z_{j\nu}(y) - \frac{1}{2\pi ik_\nu}\int dsQ_{\mu s}(y)z_{s\nu}(y)\\ &-\frac{1}{2ik_\mu}e^{-2ik_\mu y}\sum_m z_{\mu m}(y)U_{m\nu}(y)\\ &-\frac{1}{2\pi ik_\mu}e^{-2ik_\mu y}\int dpz_{\mu p}(y)U_{p\nu}(y)\\ &-\frac{1}{2ik_\mu}\frac{1}{2ik_\nu}e^{-2ik_\mu y}z_{\mu\nu}(y),\end{aligned} \quad (25)$$

subject to the boundary conditions

$$U_{\mu\nu}(y\to\infty) = 0, \quad (26)$$

$$Q_{\mu\nu}(y \to \infty) = 0. \tag{27}$$

The total probabilities of reflection and transmission in a bound state for a molecule incident in a bound state i are

$$p_{\mathrm{RB}}^{(i)} = \sum_n \frac{k_n}{k_i} |2k_i U_{ni}|^2, \tag{28}$$

$$p_{\mathrm{TB}}^{(i)} = \sum_n \frac{k_n}{k_i} |2k_i Q_{ni}|^2 + 1 - 4k_i \,\mathrm{Im}\{e^{2ik_i y} Q_{ii}\}. \tag{29}$$

The last two terms in Eq. (29) are a result of the $\delta_{\mu\nu}$ term in Eq. (23). Similarly, the total probabilities of reflection and transmission in an unbound state for a molecule incident in a bound state i are

$$p_{\mathrm{RU}}^{(i)} = \frac{1}{\pi} \int dq \frac{k_q}{k_i} |2k_i U_{qi}|^2, \tag{30}$$

$$p_{\mathrm{TU}}^{(i)} = \frac{1}{\pi} \int dq \frac{k_q}{k_i} |2k_i Q_{qi}|^2. \tag{31}$$

III. DIATOMIC MOLECULE INCIDENT UPON A δ BARRIER

A. Discrete unbound states

In this section we construct the effective potentials for a molecule incident upon a δ barrier. We first consider the case of discrete unbound states by choosing a binding potential of the form given in Eq. (6):

$$V_0(\xi) = \begin{cases} V_2, & 0 < |\xi| < a, \\ -V_1, & a < |\xi| < b, \\ 0, & b < |\xi| < L, \\ \infty, & |\xi| > L. \end{cases} \tag{32}$$

This idealized potential captures the essential physics and reduces the amount of numerical calculation by giving simple analytical expressions for the relative motion eigenfunctions. With this choice of $V_0(\xi)$ the relative motion problem given in Eqs. (4) and (5) may be solved exactly to give analytical expressions for $\chi_n(\xi)$ and $\chi_q(\xi)$.

It can be readily proven [using parity or asymptotic expansions of Eqs. (11) and (12)] that $R_{\mu\nu}=0$ and $T_{\mu\nu}=0$ if μ and ν index states of opposite parity. Physically, this means that the incident relative motion state and the reflected or transmitted relative motion state must have the same parity. Consequently, a molecule incident in an even (odd) relative motion state is calculated using only the even (odd) relative motion states. Therefore, without loss of generality, we discuss only the even states. We note that the results for a molecule incident in an odd state are similar to the results for a molecule incident in an even state. The even relative motion states are given by

$$\chi_n(\xi) = \begin{cases} A_n F_n(a)\cosh(s_n \xi), & 0 \le \xi \le a, \\ A_n \cosh(s_n a) F_n(\xi), & a \le \xi \le b, \\ A_n \sinh[r_n(L-\xi)], & b \le \xi \le L, \\ 0, & \xi \ge L, \end{cases} \tag{33}$$

$$\chi_q(\xi) = \begin{cases} A_q F_q(a)\cosh(s_q \xi), & 0 \le \xi \le a, \\ A_q \cosh(s_q a) F_q(\xi), & a \le \xi \le b, \\ A_q \sin[r_q(L-\xi)], & b \le \xi \le L, \\ 0, & \xi \ge L, \end{cases} \tag{34}$$

where

$$F_n(\xi) = \frac{\cos[p_n(b-\xi)]\sinh[r_n(L-b)]}{\cosh(s_n a)} + \frac{r_n \sin[p_n(b-\xi)]\cosh[r_n(L-b)]}{p_n \cosh(s_n a)}, \tag{35}$$

$$F_q(\xi) = \frac{\cos[p_q(b-\xi)]\sin[r_q(L-b)]}{\cosh(s_q a)} + \frac{r_q \sin[p_q(b-\xi)]\cos[r_q(L-b)]}{p_q \cosh(s_q a)}, \tag{36}$$

and

$$p_n^2 = m(V_1 + e_n)/\hbar^2, \tag{37}$$

$$r_n^2 = m(-e_n)/\hbar^2, \tag{38}$$

$$s_n^2 = m(V_2 - e_n)/\hbar^2, \tag{39}$$

$$p_q^2 = m(V_1 + e_q)/\hbar^2, \tag{40}$$

$$r_q^2 = m(e_q)/\hbar^2, \tag{41}$$

$$s_q^2 = m(V_2 - e_q)/\hbar^2. \tag{42}$$

The normalization constants A_n and A_q are lengthy expressions which are given in Appendix A. Note that even parity establishes the eigenfunctions for $\xi<0$. The eigenvalue conditions for bound and unbound states are given by

$$\frac{s_n}{p_n}\tanh(s_n a) = \frac{p_n \tan[p_n(b-a)]\tanh[r_n(L-b)] - r_n}{p_n \tanh[r_n(L-b)] + r_n \tan[p_n(b-a)]} \tag{43}$$

and

$$\frac{s_q}{p_q}\tanh(s_q a) = \frac{p_q \tan[p_q(b-a)]\tanh[r_q(L-b)] - r_q}{p_q \tanh[r_q(L-b)] + r_q \tan[p_q(b-a)]}. \tag{44}$$

By varying the parameters in the binding potential we obtain two (even) bound states, similar to the case studied in Ref. [11]. We index the even bound and unbound states in order of increasing energy, beginning with index "0," and incrementing by 2 since the states are of even parity. For the case

of two bound states we assign the indices '0' and '2' to the lower and higher energy bound states. The lowest energy unbound state is assigned the index '4', the next highest energy unbound state is indexed '6' and so on (odd states would be indexed by odd integers).

For solutions of definite parity, as in Eqs. (33) and (34), the effective potential $z_{\mu\nu}(x)$, given by Eq. (9), reduces to

$$z_{\mu\nu}(x) = \frac{4m}{\hbar^2}\int_{-\infty}^{\infty} V\left(x+\frac{1}{2}\xi\right)[1+(-1)^{\mu+\nu}]\chi_\mu^*(\xi)\chi_\nu(\xi)d\xi. \tag{45}$$

From Eq. (45) and we see that the effective potentials are symmetrical and that there is no even-odd coupling.

For the external potential barrier we choose a δ barrier of strength λ given by

$$V\left(x\pm\frac{1}{2}\xi\right) = \lambda\delta\left(x\pm\frac{1}{2}\xi\right). \tag{46}$$

This represents a δ barrier for the atoms at $x_j=0$, i.e., $V(x_j)=\lambda\delta(x_j)$ for $j=1,2$. Substituting this into Eq. (9) and integrating gives the effective potentials

$$v_{ni}(x) = \frac{16m\lambda}{\hbar^2}\chi_n^*(2x)\chi_i(2x), \tag{47}$$

$$u_{nq}(x) = \frac{16m\lambda}{\hbar^2}\chi_n^*(2x)\chi_q(2x), \tag{48}$$

$$w_{qq'}(x) = \frac{16m\lambda}{\hbar^2}\chi_q^*(2x)\chi_{q'}(2x), \tag{49}$$

where n, i index bound states and q, q' index unbound states. We have explicitly written the three cases of $z_{\mu\nu}$ above to emphasize the difference in the effective potentials. This becomes especially important in the $L\to\infty$ limit.

The definitions of the dimensionless quantities we will use are

$$\tilde{x}\equiv\frac{x}{a},\ \tilde{k}\equiv ka,\ \tilde{\lambda}\equiv\frac{\lambda}{aV_1},\ \tilde{z}_{\mu\nu}\equiv a^2 z_{\mu\nu},\ \tilde{L}\equiv\frac{L}{a},$$

$$f_n\equiv\frac{e_n}{V_1},\ f_q\equiv\frac{e_q}{V_1},\ N\equiv V_2/V_1,\ g\equiv\sqrt{\frac{mV_1}{\hbar^2}}a. \tag{50}$$

The numerical values of the dimensionless parameters are chosen to be $g=15$, $N=5$, $b/a=1.3$, $\tilde{L}=10$, and $\tilde{\lambda}=0.01$. The values of f_n calculated using Eq. (43) are $f_0=-0.7226$ and $f_2=-0.02277$. The 14 values of f_q, for the range of total molecular energies studied, are given in Appendix B. Using a as a length scale, i.e., $a=1$, we will use x, k, L, and $z_{\mu\nu}$ in place of $\tilde{x}$, $\tilde{k}$, $\tilde{L}$, and $\tilde{z}_{\mu\nu}$.

The values of the dimensionless parameters chosen above are not arbitrary, but rather have been chosen to be comparable to realistic systems. For example, taking m, V_1, and a to be on the order of an atomic mass unit, an electron volt, and the Bohr radius, respectively, one finds that g is of the same order as the value chosen above. Also, the dimensionless parameters have been chosen to give one deeply bound state and a second bound state that is also appreciably bound, i.e., the magnitude of its binding energy is not small.

B. Continuous unbound states

Taking the $L\to\infty$ limit, the relative motion eigenfunctions become

$$\chi_n(\xi) = \begin{cases} A_n^\infty F_n^\infty(a)\cosh(s_n\xi), & 0\le\xi\le a, \\ A_n^\infty \cosh(s_n a)F_n^\infty(\xi), & a\le\xi\le b, \\ A_n^\infty e^{r_n(b-\xi)}, & \xi\ge b, \end{cases} \tag{51}$$

$$\chi_q(\xi) = \begin{cases} A_q^\infty F_q^\infty(a)\cosh(s_q\xi), & 0\le\xi\le a, \\ A_q^\infty \cosh(s_q a)F_q^\infty(\xi), & a\le\xi\le b, \\ A_q^\infty \sin[r_q\xi], & \xi\ge b, \end{cases} \tag{52}$$

where

$$F_n^\infty(\xi) = \frac{\cos[p_n(b-\xi)]+(r_n/p_n)\sin[p_n(b-\xi)]}{\cosh(s_n a)}, \tag{53}$$

$$F_q^\infty(\xi) = \frac{\cos[p_q(b-\xi)]\sin[r_q b]}{\cosh(s_q a)} - \frac{r_q\sin[p_q(b-\xi)]\cos[r_q b]}{p_q\cosh(s_q a)}, \tag{54}$$

and r_n, s_n, p_n, r_q, s_q, and p_q are defined as in the case of discrete unbound states (37)–(42). The expressions for A_n^∞ and A_q^∞ are given in Appendix C. Note that even parity defines the eigenfunctions for $\xi<0$. The eigenvalue condition for bound states becomes

$$\frac{s_n}{p_n}\tanh(s_n a) = \frac{p_n\tan[p_n(b-a)]-r_n}{r_n\tan[p_n(b-a)]+p_n}, \tag{55}$$

with the values of f_n changing slightly, to $f_0=-0.7225$ and $f_2=-0.02270$.

A selected few of the dimensionless effective potentials (47)–(49), using the continuous relative motion eigenfunctions (51) and (52), are plotted in Figs. 1 and 2. A simple interpretation of the effective potentials $v_{nm}(x)$, plotted in Fig. 1, is discussed in Ref. [11]. For completeness we give a very similar description for the effective potentials $u_{nq}(x)$. Observe that the single δ barrier is transformed into the two smooth barriers of $u_{nq}(x)$ shown in Fig. 2. Specifically, $u_{0q}(x)$ is nonzero for $-1.0<x<-0.5$ and for $0.5<x<1.0$ and is effectively zero everywhere else. The reason the effective potentials are exponentially small for $-0.5<x<0.5$ is that the molecule is staggering the δ barrier, i.e., loosely speaking, one atom is on one side of the barrier and the other atom is on the other side. These two smoothly varying, nonzero regions represent the potential barrier that the center of mass encounters with the smoothness being a consequence of the integration over ξ. Recall that in one dimension the molecule encounters the barrier with one particle in front of the other. The first smooth barrier corresponds to the leading particle encountering the δ barrier and the second smooth barrier corresponds to the trailing particle encountering the δ barrier.

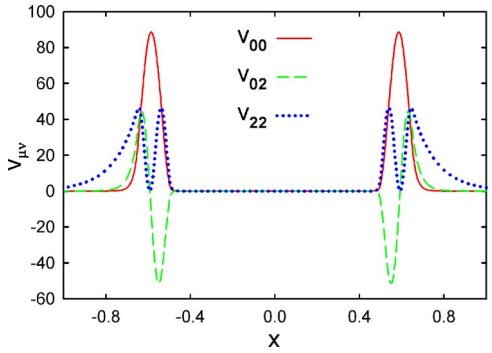

FIG. 1. (Color online) Effective potentials $v_{ni}(x)$ vs x where n and i index bound states. Note that, due to symmetry, $v_{02}(x)=v_{20}(x)$. These plots can be understood as the potential barrier that the center of mass encounters when incident upon the δ barrier in the bound state i and reflected or transmitted in the bound state n. (All quantities in all figures are dimensionless.)

The three regions, from left to right, correspond to both particles to the left of the barrier, the particles staggering the δ barrier, and both particles to the right of the barrier. These three corresponding regions for $u_{0q}(x)$ are $x<-1.0$, $-0.5<x<0.5$, and $x>1.0$.

With the effective potentials having been determined, we return to the task of calculating the probabilities of reflection and transmission. The coefficients $R_{\mu\nu}$ and $T_{\mu\nu}$ are computed using Eqs. (11) and (12) for discrete unbound states and Eqs. (24) and (25) for continuous unbound states. Transitions between internal molecular states are restricted by the total energy E. For discrete states, sums only include states with energies less than E, and for continuous states, integrals have an upper limit $q_{\max}=g\sqrt{E}$. We employ a second order backward Runge-Kutta method [15] to solve the equations while using Simpson's rule to approximate the integrals. Although solutions to multichannel equations can often lead to instabilities due to closed channel components, such instabilities were not encountered in this investigation.

Even with the substantial reduction in computation provided by the method of variable reflection and transmission amplitudes and the simplifications made above, a high performance parallel-processing computer was required to solve the equations in a reasonable amount of time. To give an appreciation of the amount of computation involved, the time required for a single 1 GHz processor to reproduce the results obtained in this paper for discrete and continuous unbound states would be on the order of months and years, respectively, whereas we obtained these results in about 20 days.

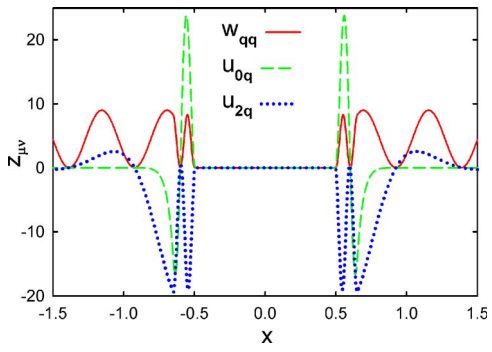

FIG. 2. (Color online) Effective potentials $u_{nq}(x)$ and $w_{qq}(x)$ vs x for $n=0,2$ and q indexes an unbound state of energy $f_q=0.05138$. Note that, due to symmetry, $u_{0q}(x)=u_{q0}(x)$ and $u_{2q}(x)=u_{q2}(x)$.

IV. RESULTS FOR A δ BARRIER

In this section we present plots of the probabilities of reflection and transmission for the molecule incident in the two bound states. In order to provide a complete description we must include plots of all four probabilities: $p_{\mathrm{RB}}^{(i)}$, $p_{\mathrm{TB}}^{(i)}$, $p_{\mathrm{RU}}^{(i)}$, and $p_{\mathrm{TU}}^{(i)}$ for $(i=0,2)$. First, we show that the results of our method for continuous states are consistent with the case of a large number of discrete states. Further, we demonstrate that even a relatively large number of discrete unbound states is not a sufficient approximation of a molecule with continuous unbound states. Next, we illustrate the effects that unbound states have on the behavior of the tunneling molecule by comparing the results for continuous unbound states to the results for a molecule without unbound states. Accordingly, we point out some of the physically intuitive features of the probability curves to help illuminate the characteristics of a molecule with unbound states. Finally, we observe the significance of the structure of the external barrier by comparing results for the molecule incident upon a δ barrier to the results obtained for rectangular and Gaussian barriers.

In Figs. 3 and 4 we compare plots of the probabilities for discrete (thin solid curve) and continuous (heavy solid curve) unbound states. Figure 3 features plots of $p_{\mathrm{RU}}^{(0)}$ and $p_{\mathrm{TU}}^{(0)}$ for the molecule incident in the ground state while Fig. 4 features plots of $p_{\mathrm{RU}}^{(2)}$ and $p_{\mathrm{TU}}^{(2)}$ for the molecule incident in the excited state. The plots are presented over a range of k_0 in the unbound regime which starts at $k_0\approx 25.5$, as given by Eq. (10). Note that for $k_0<25.5$, $p_{\mathrm{TB}}^{(i)}\equiv p_T^{(i)}$, $p_{\mathrm{RB}}^{(i)}\equiv p_R^{(i)}$, and $p_{\mathrm{TU}}^{(i)}=p_{\mathrm{RU}}^{(i)}=0$ for $(i=0,2)$. An immediate observation is the lack of resonant structure in the probabilities of reflection and transmission in unbound states. By this we mean that the probabilities are neither zero nor unity throughout the range of k_0 shown in Figs. 3 and 4. It will be shown that this feature of the probabilities of reflection and transmission in unbound states results in a significant reduction in the transmission resonances observed for a molecule without unbound states, reported in Ref. [11].

The erratic fluctuations of the curves for discrete unbound states is the result of the unbound energies being discrete. More specifically, $p_{\mathrm{RU}}^{(i)}$ and $p_{\mathrm{TU}}^{(i)}$ increase sharply as each additional discrete unbound state is made available energetically because each additional unbound state provides more ways in which the molecule can break up. The superposition of these sharp peaks, and their subsequent oscillations, causes the complicated structure seen in the figures. Note that the values of k_0 at which the unbound states (listed in Appendix B) become energetically accessible can be calculated using Eq. (10) with e_q in place of E. The curves for

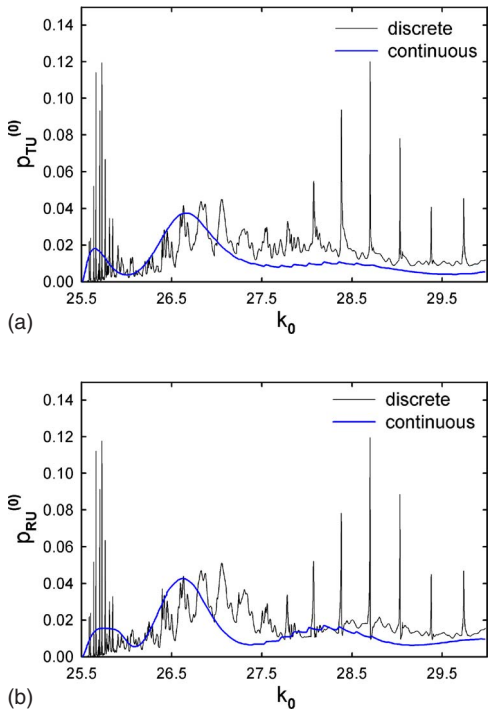

FIG. 3. (Color online) $p_{\mathrm{TU}}^{(0)}$, $p_{\mathrm{RU}}^{(0)}$ vs k_0 for a range of k_0 in the unbound regime, which begins at $k_0 \approx 25.5$. Shown are the probabilities for continuous unbound states (heavy curve) and discrete unbound states (light curve) with $L=10$. The top figure features the probability of transmission in unbound states while the bottom figure features the probability of reflection in unbound states, for the molecule incident in the ground state.

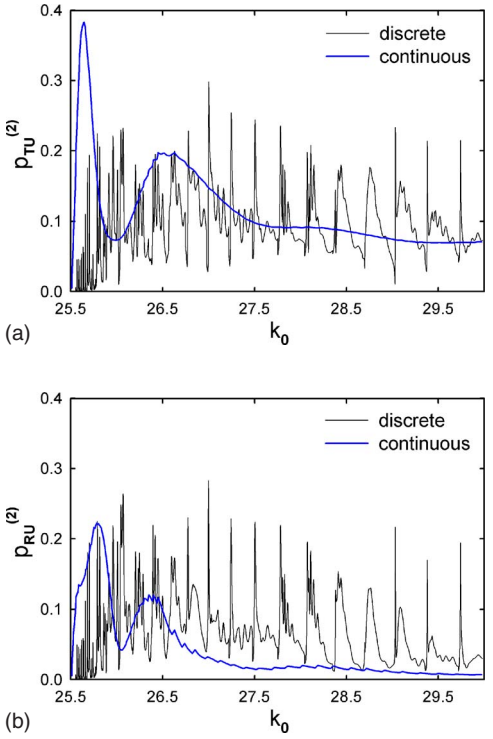

FIG. 4. (Color online) $p_{\mathrm{TU}}^{(2)}$, $p_{\mathrm{RU}}^{(2)}$ vs k_0 for a range of k_0 in the unbound regime, which begins at $k_0 \approx 25.5$. Shown are the probabilities for continuous unbound states (heavy curve) and discrete unbound states (light curve) with $L=10$.

continuous unbound states follow the general trends of the curves for discrete unbound states supporting the validity of the continuous unbound state equations derived in Sec. II B.

Although the results for $L=10$ are in agreement with the results for continuous unbound states, they clearly could not be used to effectively approximate the continuous unbound state results. We found that 15 discrete unbound states is close to the practical limit for numerical solution. Since the amount of computation required to produce the results for discrete unbound states increases exponentially as the number of states increases it appears to be computationally infeasible to use discrete states to model a molecule with continuous unbound states.

Notice that in Figs. 3 and 4, $p_{\mathrm{RU}}^{(i)}$ and $p_{\mathrm{TU}}^{(i)}$ are significantly larger for the molecule incident in the excited state ($i=2$) than in the ground state ($i=0$). The excited molecule is more unstable, being closer in energy to the unbound states, making it much more likely to break up. Also, for $k_0 > 27.5$, $p_{\mathrm{RU}}^{(2)} \approx 0.007$ is a factor of 10 less than $p_{\mathrm{TU}}^{(2)} \approx 0.07$. In other words, for the molecule incident in the excited state with a large kinetic energy, the probability of reflection in an unbound state is much less than the probability of transmission in an unbound state. This is in consequence of the general feature that the total probability of reflection tends to zero as the energy of the molecule increases. This necessitates that both $p_{\mathrm{RB}}^{(2)}$ and $p_{\mathrm{RU}}^{(2)}$ must also tend to zero while the probability of transmission does not have such a restriction.

In Figs. 5 and 6 the effect of the inclusion of continuous unbound states is demonstrated. We compare the total probabilities of reflection and transmission for a molecule with continuous unbound states (dashed curves) to those of a molecule with no unbound states (solid curves). Note that the results for a molecule without unbound states were reported in Ref. [11]. Also included in Figs. 5 and 6 are the probabilities of reflection and transmission in only bound states (dotted curves) for the molecule with continuous unbound states. The curves for which unbound states are included (dashed curves) share the same overall structure as the curves for which unbound states are not included (solid curves). This indicates that, for the parameters chosen in this investigation, the bound states dominate much of the behavior of the molecule in the process of tunneling. Another perspective of the same observation is the agreement between the curves for total reflection and transmission (dashed curves) and reflection and transmission in only bound states (dotted curves). As a result, the analysis developed and used in Ref. [11], in which there were no unbound states, could still be used to estimate the basic features of the probability curves for when unbound states are included, such as the locations of the maxima and minima and overall trends.

The unbound states result in a significant physical feature. They are responsible for reducing the probability of transmission and thus turning the transmission resonances, observed for the case of a molecule without unbound states, into quasiresonances. Of particular interest are the reductions in the probability of transmission in a bound state. These

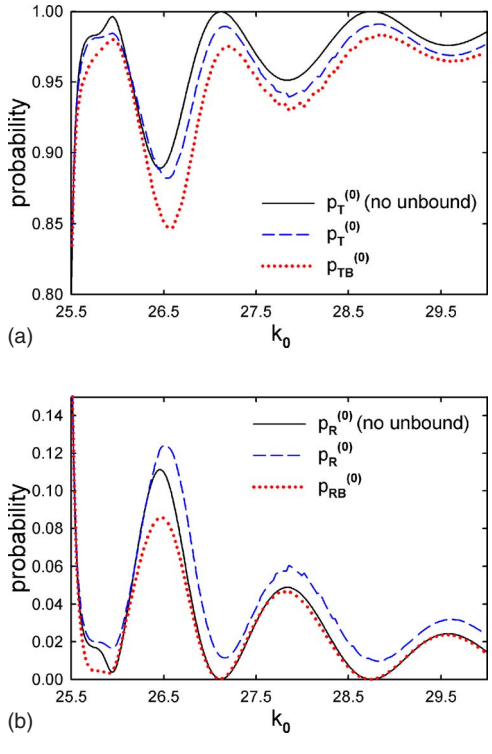

FIG. 5. (Color online) $p_R^{(0)}$, $p_T^{(0)}$ vs k_0 comparing a molecule with continuous unbound states (dashed curves) to a molecule without unbound states (solid curves). Also included are $p_{\mathrm{RB}}^{(0)}$ and $p_{\mathrm{TB}}^{(0)}$ vs k_0 (dotted curves); i.e., the probabilities of reflection and transmission in bound states only for a molecule with continuous unbound states.

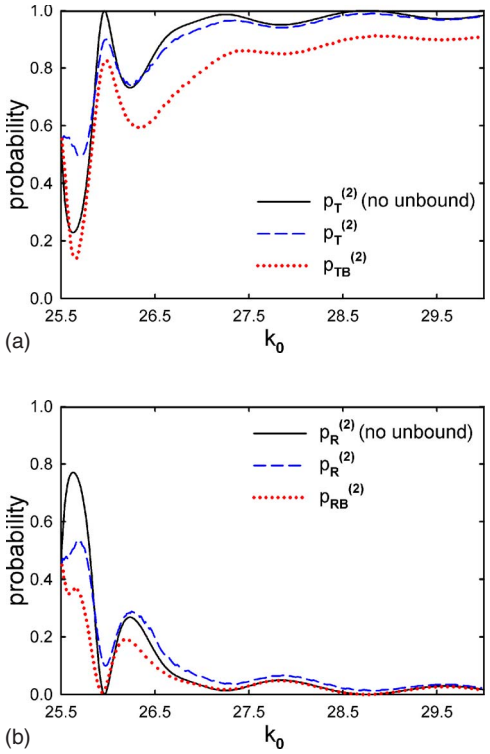

FIG. 6. (Color online) $p_R^{(2)}$, $p_T^{(2)}$ vs k_0 comparing a molecule with continuous unbound states (dashed curves) to a molecule without unbound states (solid curves). Also included are $p_{\mathrm{RB}}^{(2)}$ and $p_{\mathrm{TB}}^{(2)}$ vs k_0 (dotted curves); i.e., the probabilities of reflection and transmission in bound states only for a molecule with continuous unbound states.

reductions are highlighted in Fig. 7. The reason that $p_{\mathrm{TB}}^{(i)}$ is reduced when unbound states are taken into account is that $p_{\mathrm{RU}}^{(i)}$ and $p_{\mathrm{TU}}^{(i)}$ are nonzero throughout the range of k_0 shown in Figs. 3 and 4. For the molecule incident in the ground state, $p_T^{(0)}$ (no unbound) has two resonances located at $k_0 \approx 27.12$ and $k_0 \approx 28.75$. We will temporarily refer to these two resonances as the lower and higher energy resonances, respectively. Even though $p_{\mathrm{RB}}^{(0)}$ approaches zero at these two points $p_{\mathrm{RU}}^{(0)} \approx 0.011$ and $p_{\mathrm{TU}}^{(0)} \approx 0.016$ at the lower energy resonance while $p_{\mathrm{RU}}^{(0)} \approx 0.010$ and $p_{\mathrm{TU}}^{(0)} \approx 0.0089$ at the higher energy resonance. This accounts for the fact that when continuous unbound states are included, the probability of transmission in a bound state $p_{\mathrm{TB}}^{(0)}$ is reduced from unity by approximately 0.027 and 0.019 at the lower and higher energy resonances, respectively. These reductions are certainly significant considering that the differences between neighboring maxima and minima are approximately 0.12, 0.045, and 0.019.

For the molecule incident in the excited state, the reductions in the probability of transmission at the points of resonance are even more substantial. The resonance located at $k_0 = 25.96$ in Fig. 7 is reduced by 0.18, which is also comparable to the difference between the maximum and minimum values in the region. Furthermore, for $k_0 > 26.5$ there is a fairly constant, sizeable difference (as much as 0.20) between $p_{\mathrm{TB}}^{(2)}$ and $p_T^{(2)}$ (no unbound). This difference is a result of the relatively large probability of transmission in an unbound state for large kinetic energy as discussed before.

Another pronounced change is in the total probability of tunneling for the molecule incident in the excited state. As shown in Fig. 6, for $25.5 < k_0 < 26.1$ the difference between $p_T^{(2)}$ and $p_T^{(2)}$ (no unbound) is as much as 0.30. This is due to the high probability of transmission in an unbound state in this region as seen in Fig. 4. We conclude that the inclusion of unbound states has a significant effect on probability of tunneling, especially at the points of resonance, and therefore the inclusion of unbound states is essential for a satisfactory understanding of molecular tunneling.

V. RESULTS FOR RECTANGULAR AND GAUSSIAN BARRIERS

The influence of the structure of the external barrier on the probabilities of reflection and transmission can be appreciated by considering the molecule incident upon other types of barriers. We study a rectangular barrier given by

$$V(x) = \begin{cases} 0, & |x| > w/2, \\ V_r, & |x| < w/2, \end{cases} \tag{56}$$

and a Gaussian barrier given by

$$V(x) = \frac{A}{\sigma\sqrt{2\pi}} \exp\left(-\frac{x^2}{2\sigma^2}\right), \tag{57}$$

from which the effective potentials $z_{\mu\nu}$ can be calculated numerically.

In Figs. 8 and 9, the probabilities of transmission through rectangular and Gaussian barriers are compared to the results

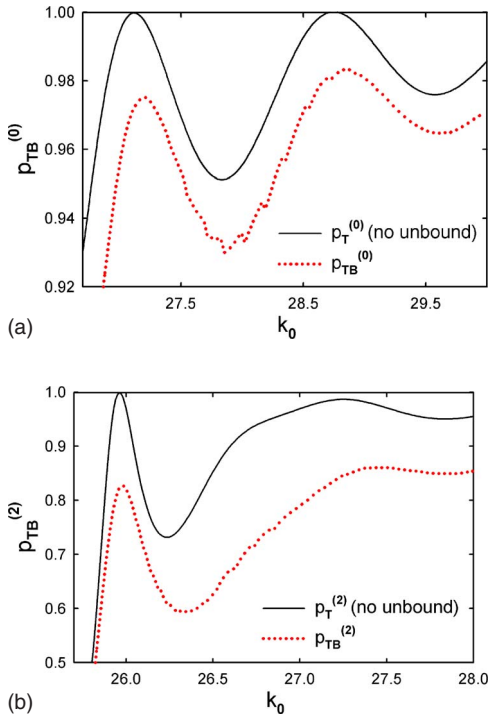

FIG. 7. (Color online) $p_{\mathrm{TB}}^{(i)}$ vs k_0 for $i=(0,2)$ comparing a molecule with continuous unbound states (dotted curve) to a molecule without unbound states (solid curve). Note that for a molecule with no unbound states $p_{\mathrm{TB}}^{(i)} \equiv p_T^{(i)}$. The reduction in the resonances, due to inclusion of the unbound states, are about 0.027 and 0.18 for the molecule incident in the ground and excited states, respectively.

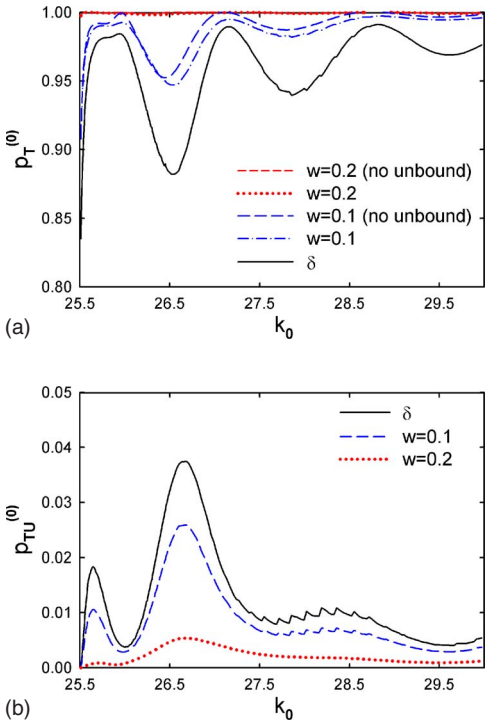

FIG. 8. (Color online) $p_T^{(0)}$ and $p_{\mathrm{TU}}^{(0)}$ vs k_0 for rectangular barriers. Rectangular barriers of widths $w=0.1$ and $w=0.2$ are investigated with the condition $V_r w=\tilde{\lambda}=0.01$, where V_r is the height of the barrier. The top figure compares $p_T^{(0)}$ for each rectangular barrier with unbound states, to the corresponding case without unbound states. Also included is $p_T^{(0)}$ for the δ barrier. Note that $p_T^{(0)}$ for $w=0.2$ is very close to 1. The bottom figure compares $p_{\mathrm{TU}}^{(0)}$ for the rectangular barriers and the δ barrier.

given above for the δ barrier. Note that the areas of the rectangular and Gaussian barriers are equal to the strength of the δ barrier. Also note that the figures for the rectangular barriers are similar to the figures for the Gaussian barriers, but they are not identical. The chosen values of $w=w/a$ and $\sigma=\sigma/a$ are rather large to show the deviations from the δ barrier and we note that for $w<0.1$ and $\sigma<0.03$, the agreement between rectangular, Gaussian, and δ barriers is excellent. We point out that larger values of w and σ produce potential barriers that are lower in energy and are spread over longer distances. Therefore, for narrow and tall barriers, one can be confident that the δ barrier will capture the important physics of the molecular tunneling reported in this paper.

We note that a comparison of the probabilities of reflection are exceedingly similar to the comparisons of the probabilities of transmission shown in Figs. 8 and 9. Furthermore, for the molecule incident in the excited state $p_{\mathrm{RU}}^{(2)}$ and $p_{\mathrm{TU}}^{(2)}$ for the various rectangular and Gaussian barriers investigated were all in excellent agreement with the δ barrier (almost identical).

VI. EXTENSIONS TO MORE REALISTIC SYSTEMS

An obvious extension of the results in this paper is from one dimension into three dimensions. Consideration of the rotational and vibrational modes of a tunneling molecule with only bound states has been investigated in Ref. [12]. It was found that there are many differences between the main features of a molecule tunneling in one dimension versus three dimensions. The freedom associated with the rotational modes allows for orientations of the axis of the molecule which are not perpendicular to the barrier. Consequently, the structure of the effective potentials in three dimensions are incommensurable to those in one dimension resulting in the distinctive probabilities curves. However, many of the characteristics observed in this one-dimensional study will be constituent in a three-dimensional investigation. We expect that the differences between a molecule with and without unbound states in three dimensions will be similar to the differences observed in one dimension.

Additional considerations of the already complex internal structure of the diatomic molecule could be investigated. It has been shown that the probability of transmission for a bound pair incident upon a potential barrier is considerably different when the internal structure (e.g., spin) of the pair is taken into account [8]. A fully realistic treatment of the tunneling of a diatomic molecule will have to acknowledge this property in its formalism.

It has been demonstrated that it is possible to align molecules in a molecular beam using laser pulses, optical fields, dc electric fields, and inhomogeneous electric fields [16]. Such methods might permit a situation in which the results of this paper could be applied in an experimental setting.

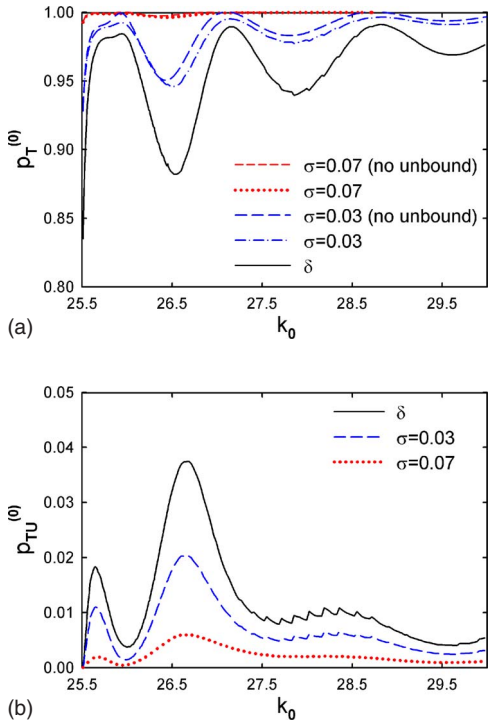

FIG. 9. (Color online) $p_T^{(0)}$ and $p_{\mathrm{TU}}^{(0)}$ vs k_0 for Gaussian barriers. Gaussian barriers with parameters $\sigma=0.03$ and $\sigma=0.07$ are investigated with the total area of the barrier $A=\tilde{\lambda}=0.01$. The top figure compares $p_T^{(0)}$ for each Gaussian barrier with unbound states, to the corresponding case without unbound states. Also included is $p_T^{(0)}$ for the δ barrier. Note that $p_T^{(0)}$ for $\sigma=0.07$ is very close to 1. The bottom figure compares $p_{\mathrm{TU}}^{(0)}$ for the Gaussian barriers and the δ barrier.

This work also has applications in the tunneling of excitons. For example, Saito and Kayanuma studied the tunneling of a ballistic Wannier exciton though a single-barrier heterostructure [17]. It was found that the exciton exhibits tunneling resonances by the same mechanism as discussed in previous papers on the tunneling of diatomic molecules [11,12]. The results in this paper also apply to such investigations in the tunneling of excitons [18].

The relationship between scattering and tunneling problems provides many additional examples of applications in molecular physics. The scattering of H_2 from Cu(001) [19] and NO from diamond (110) [20] have been shown to produce energy resonances analogous to those presented in this one-dimensional model. Furthermore, it has been shown that the scattering distributions depend on the incoming and outgoing states (i.e., vibrational and rotational excitations) similar to the internal excitations included in our model.

VII. SUMMARY

The probabilities of reflection and transmission in bound and unbound states were calculated with the inclusion of discrete and continuous unbound states. The results for continuous unbound states were found to be in reasonable agreement with results for a large number of discrete unbound states, but the number of discrete unbound states required to effectively approximate a continuum would be computationally impractical.

The inclusion of unbound states revealed significant changes. Most importantly, the transmission resonances observed for a molecule without unbound states were found to be considerably reduced when unbound states were included. This was due to the probabilities of reflection and transmission in unbound states lacking resonant structure, i.e., the probabilities of reflection and transmission in unbound states were nonzero throughout the energy range investigated. Consequently, the probabilities of transmission in a bound state at the points of resonance were found to be reduced by as much as 2.7% and 18% for the molecule incident in the ground and excited states, respectively. These reductions were especially significant compared to the largest differences between maxima and minima in this energy range. Also, for the molecule incident in the excited state, the total probability of transmission was found to increase by more than 30%. This was a result of the high probability of transmission in an unbound state in that region. Furthermore, a large (approximately 20%) and fairly constant reduction in the probability of transmission in bound states was observed for the molecule incident in the excited state. This was again due to high probabilities of transmission in unbound states. Such examples show that the inclusion of unbound states is crucial in many cases, and especially so at the points of resonance.

It was also found that the bound states were more influential than the unbound states in the process of tunneling. That is, the main features of the probability curves were preserved when unbound states were included. For example, the locations of the maxima and minima of the probability curves changed only slightly. Consequently, the analysis developed and used in Ref. [11] could still be used to estimate the general trends of the probability curves for when unbound states are included.

The significance of the structure of the barrier was investigated by comparing the results for a δ barrier to rectangular and Gaussian barriers. The results for the δ barrier were found to be in excellent agreement with results for narrow rectangular and Gaussian barriers. Surprisingly, the δ barrier was also found to be in reasonable agreement with considerably wide rectangular and Gaussian barriers. This indicates that the δ barrier captures the essential physics of molecular tunneling past a high energy, spatially narrow potential barrier.

The work reported here for one dimension is currently being extended to three dimensions. Further considerations such as additional internal structure and increasing commensurability to realistic systems will be topics for future investigations.

ACKNOWLEDGMENTS

This work was supported by the Natural Sciences and Engineering Research Council of Canada (NSERC). We thank Professor M. Razavy, Mr. Glen Goodvin, and Mr. John Koblanski for helpful discussions. We also thank Dr. Y. Q.

Wang for assistance with the use of the High Performance Computing (HPC) facility at the University of Northern British Columbia.

APPENDIX A: RELATIVE MOTION NORMALIZATION CONSTANTS FOR DISCRETE UNBOUND STATES

The bound and unbound normalization constants are, respectively, given by

$$A_n = \frac{1}{2}\left[\frac{\Gamma_n}{p_n} + \frac{\Omega_n}{r_n} + \frac{\Theta_n^2\Phi_n}{s_n}\right]^{-1/2}, \tag{A1}$$

$$A_q = \frac{1}{2}\left[\frac{\Gamma_q}{p_q} - \frac{\Omega_q}{r_q} + \frac{\Theta_q^2\Phi_q}{s_q}\right]^{-1/2}, \tag{A2}$$

where

$$\Gamma_n = \alpha_n\left[\sinh^2(\beta_n) + \frac{r_n^2}{p_n^2}\cosh^2(\beta_n)\right] + \sin^2(\alpha_n)\left[2\frac{r_n}{p_n}\sinh(\beta_n)\cosh(\beta_n)\right] + \sin(\alpha_n)\cos(\alpha_n)\left[\sinh^2(\beta_n) - \frac{r_n^2}{p_n^2}\cosh^2(\beta_n)\right], \tag{A3}$$

$$\Omega_n = \sinh(\beta_n)\cosh(\beta_n) - \beta_n, \tag{A4}$$

$$\Theta_n = \cos(\alpha_n)\sinh(\beta_n) + \frac{r_n}{p_n}\sin(\alpha_n)\cosh(\beta_n), \tag{A5}$$

and

$$\Gamma_q = \alpha_q\left[\sin^2(\beta_q) + \frac{r_q^2}{p_q^2}\cos^2(\beta_q)\right] + \sin^2(\alpha_q)\left[2\frac{r_q}{p_q}\sin(\beta_q)\cos(\beta_q)\right] + \sin(\alpha_q)\cos(\alpha_q)\left[\sin^2(\beta_q) - \frac{r_q^2}{p_q^2}\cos^2(\beta_q)\right], \tag{A6}$$

$$\Omega_q = \sin(\beta_q)\cos(\beta_q) - \beta_q, \tag{A7}$$

$$\Theta_q = \cos(\alpha_q)\sin(\beta_q) + \frac{r_q}{p_q}\sin(\alpha_q)\cos(\beta_q), \tag{A8}$$

and (for $\nu = n, q$)

$$\Phi_\nu = \frac{\sinh(\epsilon_\nu)\cosh(\epsilon_\nu) + \epsilon_\nu}{\cosh^2(\epsilon_\nu)}, \tag{A9}$$

$$\alpha_\nu = p_\nu(b-a), \tag{A10}$$

$$\beta_\nu = r_\nu(L-b), \tag{A11}$$

$$\epsilon_\nu = s_\nu a. \tag{A12}$$

APPENDIX B: DISCRETE UNBOUND RELATIVE MOTION EIGENVALUES

The values of $f_q \equiv e_q/V_0$ calculated using Eq. (44) for the chosen parameters are $f_2=0.0006234$, $f_4=0.002487$, $f_6=0.005575$, $f_8=0.009865$, $f_{10}=0.01534$, $f_{12}=0.02198$, $f_{14}=0.02979$, $f_{16}=0.03874$, $f_{18}=0.04884$, $f_{20}=0.06008$, $f_{22}=0.07246$, $f_{24}=0.08598$, $f_{26}=0.1006$, $f_{28}=0.1164$, and $f_{30}=0.1334$.

APPENDIX C: RELATIVE MOTION NORMALIZATION CONSTANTS FOR CONTINUOUS UNBOUND STATES

We present the continuous unbound state constants in a form analogous to the discrete unbound state constants for ease of use as well as for clarity in the $L\to\infty$ limit. The bound and unbound normalization constants are, respectively, given by

$$A_n^\infty = \frac{1}{2}\left[\frac{\Gamma_n^\infty}{p_n} + \frac{\Omega_n^\infty}{r_n} + \frac{(\Theta_n^\infty)^2\Phi_n}{s_n}\right]^{-1/2}, \tag{C1}$$

$$A_q^\infty = \frac{1}{2}, \tag{C2}$$

where

$$\Gamma_n^\infty = \alpha_n\left[1 + \frac{r_n^2}{p_n^2}\right] + \sin^2(\alpha_n)\left[2\frac{r_n}{p_n}\right] + \sin(\alpha_n)\cos(\alpha_n)\left[1 - \frac{r_n^2}{p_n^2}\right], \tag{C3}$$

$$\Omega_n^\infty = 1, \tag{C4}$$

$$\Theta_n^\infty = \cos(\alpha_n) + \frac{r_n}{p_n}\sin(\alpha_n); \tag{C5}$$

Φ_n, α_n, and ϵ_n are defined in Appendix A.

[1] L. J. Lauhon and W. Ho, Phys. Rev. Lett. **85**, 4566 (2000).
[2] J. J. Toppari, T. Kühn, A. P. Halvari, J. Kinnunen, M. Leskinen, and G. S. Paraoanu, Phys. Rev. B **76**, 172505 (2007).
[3] M. Albiez, R. Gati, J. Fölling, S. Hunsmann, M. Cristiani, and M. K. Oberthaler, Phys. Rev. Lett. **95**, 010402 (2005).
[4] N. Saito and Y. Kayanuma, J. Phys.: Condens. Matter **6**, 3759 (1994).
[5] F. M. Pen'kov, J. Exp. Theor. Phys. **91**, 698 (2000).
[6] F. M. Pen'kov, Phys. Rev. A **62**, 044701 (2000).
[7] V. L. Bulatov and P. E. Kornilovitch, Europhys. Lett. **71**, 352

(2005).
[8] C. A. Bertulani, V. V. Flambaum, and V. G. Zelevinsky, J. Phys. G **34**, 2289 (2007).
[9] S. Bacca and H. Feldmeier, Phys. Rev. C **73**, 054608 (2006).
[10] Y. J. Lee, J. Korean Phys. Soc. **49**, 103 (2006).
[11] G. L. Goodvin and M. R. A. Shegelski, Phys. Rev. A **71**, 032719 (2005).
[12] G. L. Goodvin and M. R. A. Shegelski, Phys. Rev. A **72**, 042713 (2005).
[13] M. Razavy, *Quantum Theory of Tunneling* (World Scientific, Singapore, 2003).
[14] B. Jackson, Annu. Rev. Phys. Chem. **46**, 251 (1995).
[15] J. Stoer and R. Bulirsch, *Introduction to Numerical Analysis*, 2nd ed. (Springer-Verlag, New York, 1992).
[16] T. P. Rakitzis, A. J. van den Brom, and M. H. M. Janssen, Science **303**, 1852 (2004).
[17] N. Saito and Y. Kayanuma, Phys. Rev. B **51**, 5453 (1995).
[18] H. Jin, L. J. Zhang, Z. H. Zheng, X. G. Kong, L. N. An, and D. Z. Shen, Acta Phys. Sin. **53**, 3211 (2004), and references therein.
[19] Y. Miura, W. A. Dino, H. Kasai, and A. Okiji, J. Phys. Soc. Jpn. **69**, 3878 (2000).
[20] C. Roth, J. Hager, and H. Walther, J. Chem. Phys. **97**, 6880 (1992).